Geoderma 334 (2019) 124–133

Contents lists available at ScienceDirect

Geoderma

journal homepage: www.elsevier.com/locate/geoderma

Baseline map of soil organic carbon in Tibet and its uncertainty in the 1980s

Y. Zhou[a], R. Webster[b], R.A. Viscarra Rossel[c], Z. Shi[a,d,*], S. Chen[e]

[a] College of Environmental and Resource Sciences, Zhejiang University, Hangzhou, China
[b] Rothamsted Research, Harpenden AL5 2JQ, UK
[c] CSIRO, PO Box 1666, Canberra, ACT 2601, Australia
[d] State Key Laboratory of Soil and Sustainable Agriculture, Institute of Soil Science, Chinese Academy of Sciences, Nanjing, China
[e] INRA, Unité Infosol, Orléans 45075, France

ARTICLE INFO

Handling Editor: A.B. McBratney

Keywords:
Soil organic carbon
Digital soil mapping
Tibetan Plateau
Soil carbon stock
Climate change

ABSTRACT

Much of the carbon (C) stored in the soil of the high Qinghai–Tibet Plateau could be lost as a result of global warming. To provide a baseline against which to assess the loss we have made a new map at 90-m resolution from sample data of 1148 soil profiles augmented by information on climate, vegetation, physiography and digital elevation. We used the program Cubist, which works as a form of regression tree, to predict the concentration at the nodes of the 90-m grid. The uncertainty of the predictions was computed by bootstrapping 50 times at each node. Soil type, evapotranspiration (ET), precipitation, radiation and vegetation type contributed most to the variation in C at the coarse scale; temperature, net primary productivity, normalized difference vegetation index (NDVI), ET and elevation contributed most at finer scales. We mapped the predicted concentration of C and converted the predictions to stocks of C for the main kinds of land: 1.93 Pg for the alpine steppe, 1.57 Pg for the meadow, 0.66 Pg in the coniferous forest, 0.63 Pg in the broadleaf forest, 1.06 Pg under shrub, < 0.4 Pg for each of the alpine desert and cropland. We estimate the uppermost 30 cm of soil to contain 6.81 Pg of C with 95% (3.80 to 10.27 Pg). This estimate differs substantially from the two previous coarser estimates based on global modelling which far exceed our 95% upper confidence limit. Our new estimate can now serve as a base against which to judge any change of soil C as a response to global warming.

1. Introduction

Soil contains more carbon than the rest of the terrestrial biosphere and plays a vital role in the global carbon cycle. We now realize that the soil's organic carbon in particular is increasingly important in the behaviour of ecosystems, both natural and agricultural. If the soil were to sequester more carbon it would help to mitigate the effects of emissions of the greenhouse gases to the atmosphere from fossil fuel, and simultaneously it should improve the quality and productivity of the soil to provide food (Nadeu et al., 2015). Alternatively, loss of carbon from the soil would exacerbate the effects. Nearly one quarter of the earth's land is mountain where loss of carbon from the soil could have serious consequences for global climate warming and ecological functioning (Kapos et al., 2000; Yang et al., 2008). Carbon stored in the soil of world's mountain grasslands and shrub lands is estimated to be between 60.5 and 82.8 Pg (Ward et al., 2014); this is one of the most important reservoirs of carbon.

Many investigators have studied the characteristics and controls of organic matter in the soil of high ecosystems and monitored changes in them. Nevertheless, the difficulties of studying at such high altitudes and the heterogeneity of the landscapes mean that our knowledge of the amount of carbon stored and its patterns of distribution remains very uncertain (Liu et al., 2012).

The Qinghai–Tibet Plateau, familiarly known as 'the roof of the world', with an area of 2 500 000 km^2 and an average altitude of 4500 m, is the largest ecosystem at this height on earth. Much of it is underlain by permafrost in which stored C is inactive. Of general concern is that with global warming some or all of the permafrost will melt, making the carbon available to microbial attack and the release of CO_2 into the atmosphere (Ding et al., 2016). The topography of the Plateau is far from flat; rather it is complex. In southeastern Tibet, for example, the land falls more than 500 m within 1 km in valleys. Such dramatic change in height is accompanied by substantial variation in the soil.

Despite the complexity of the land form, the Plateau is an ideal region for studying the effects of climate on the soil's organic carbon. Unlike lower lands, it has scarcely been disturbed by human activity. Nevertheless, the difficulties of access and logistics for sampling on the Plateau's mean that there have been few attempts to estimate and map

* Corresponding author.
E-mail address: shizhou@zju.edu.cn (Z. Shi).

https://doi.org/10.1016/j.geoderma.2018.07.037
Received 5 December 2017; Received in revised form 22 July 2018; Accepted 27 July 2018
Available online 07 August 2018
0016-7061/

the soil's organic C content there (Dörfer et al., 2013, Ma et al., 2016; Yang et al., 2016) and very few for the whole of the Plateau. Those studies have focused on specific vegetation or soil types such as grasslands and permafrost. Further, sampling has been sparse compared with those studies in other mountain area (Ballabio, 2009; Hoffmann et al., 2014). For example, Yang et al. (2016) predicted the organic in the soil of approximately 30 000 km^2 from a sample of only 99 points, and Yang et al. (2008) estimated the stock of C in Tibetan grasslands, which cover 60% of the total plateau (approximately 1 200 000 km^2) from data of 405 soil profiles. Most of our understanding on the spatial distribution and temporal dynamics of organic C in the soil is from research on individual landscapes and small regions or on single forms of land cover.

To improve our understanding of the effects of height on the distribution of the soil's organic C across the Plateau we need maps at fine resolution of both carbon content and its uncertainty.

There are several global soil maps, such as the harmonized world soil database (HWSD) (FAO/IIASA/ISRIC/ISSCAS/JRC, 2012), SoilGrids1 km (Hengl et al., 2014) and SoilGrids250 m (Hengl et al., 2017) and currently the GlobalSoilMap (Arrouays et al., 2014) with at a 3 arc-second resolution. We, however, are concerned specifically with the Qinghai–Tibet Plateau, and the aim of the research we report here was to map at 90-m resolution of the concentration of organic C in the soil of the Plateau. This would provide a baseline against which to assess future change. We pursued our aim by collating the most comprehensive currently available data on the the soil's content of organic C from the Plateau and building a soil–landscape model with multiple environmental co-variables by data-mining.

2. The study region

Our study region is the Tibet Autonomous Region (Tibet for short hereafter),78 ° 25′ N and 99° 06′ E and 26° 50′ and 36° 53′ N, which is the main component of the Qinghai–Tibet Plateau, covering more than 120 000 km^2 (Fig. 1a). A large proportion of the land (86%) exceeds 4000 m above sea level, and somewhat more than half (53%) lies above 5000 m. However, because of the logistic difficulties mentioned above we have concentrated our effort on one part of the Plateau, namely the Sygera Mountain (Fig. 1a).

The Sygera Mountain is one of the most accessible parts of Tibet, and we have been able to study its soil and environment in some detail. It hosts several types of vegetation that occur elsewhere on the Plateau. These include agricultural crops in the fertile valleys at the foot on the mountain and broad-leaved forests at mid-altitudes(mainly below 2500 m). Above them in sequence of increasing altitude are coniferous forests, shrubs and finally alpine meadows above 4500 m. The Mountain's climate is somewhat wetter than elsewhere with annual precipitation of approximately 676 mm. Its mean monthly temperatures range from 0.5 to 15.8 °C. We regard it as typical sub-humid alpine caused by the South Asian monsoon which approaches through the valley of the Brahmaputra River. There is, however, a trend from warm and humid in the south east to colder and drier in the north west.

3. Methods

3.1. Soil depth functions to derive estimates of organic C in the 0–30 cm layer

We wanted to predict the concentration of organic C in the uppermost 30 cm of the soil. The data from the National Soil Survey of China are recorded by soil horizons at various intervals in the profiles. To predict from such data we used the equal-area smoothing spline developed by Bishop et al. (1999) and Malone et al. (2009) to describe the way the concentration of C varies down the profile. This is obtained as follows.

We denote the depths of the lower boundaries of the layers in any given soil profile by $x_i, i = 0,1,2,\ldots,n$, such that $x_0 < x_1 < x_2,\ldots, < x_n$. We associate with each layer i a corresponding value of the soil property y of interest as y_i. We then model y as

$$y_i = \overline{f_i} + \varepsilon_i \quad (1)$$

where $\overline{f_i}$ is the mean value of y at depth between x_{i-1} and x_i, and ε_i is a measurement error with a mean of 0 and a variance of σ^2. We denote $f(x)$ as the spline function of the soil property at depth x, which we find by minimizing

$$f(x) = \frac{1}{n}\sum_{n=1}^{n}(y_i - \overline{f_i})^2 + \lambda\int_{x_0}^{x_n}\{f'(x)\}^2 dx \quad (2)$$

where the first term on the right-hand side represents the fit of the spline to the data and the second term expresses the roughness of the function $f(x)$. The parameter λ controls the trade-off between the fit and the roughness of the spline. Bishop et al. (1999) and Malone et al.

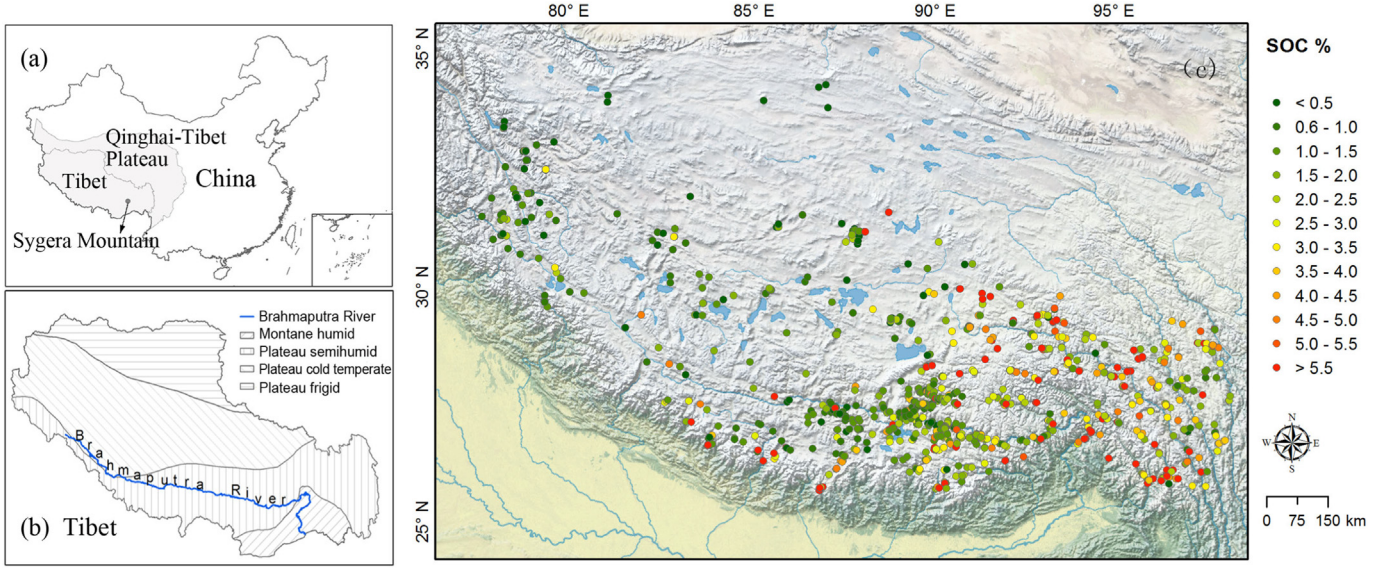

Fig. 1. Spatial distribution of soil samples used for modelling and validation. (a) Presents the location of Tibet, Sygera Mountain, Qinghai-Tibet Plateau and China. (b) Presents the climate zone in Tibet and the Brahmaputra River, and (c) Presents the soil samples we collected in Tibet.

Table 1
Environmental factors used for spatial modelling.

Theme	Environmental factors	Original resolution	Source
Soil	Soil type	1:1 000 000	Shi et al. (2004)
	Geology	1:4 000 000	Chinese Academy of Sciences (2001)
	Silt content	1 km	Shangguan et al. (2012)
	Sand content	1 km	Shangguan et al. (2012)
	Clay content	1 km	Shangguan et al. (2012)
Climate	Temperature		RESDC (2016)
	Land surface temperature of daytime	1 km	NASA Land Processes Distributed Active Archive Center (2001)
	Land surface temperature of night	1 km	NASA Land Processes Distributed Active Archive Center (2001)
	TRMM	1 km	Ma et al. (2017)
	Prescott	1 km	Prescott (1950)
	Radiation	1 km	Lu et al. (2010)
Organism	NDVI	250 m	NASA Land Processes Distributed Active Archive Center (2001)
	NPP	500 m	NASA Land Processes Distributed Active Archive Center (2001)
	ET	500 m	NASA Land Processes Distributed Active Archive Center (2001)
	Vegetation type	1 km	Chinese Academy of Sciences (2001)
Terrain	DEM	90 m	USGS (2006)
	Terrain roughness index	90 m	USGS (2006)
	Terrain wetness index	90 m	USGS (2006)
	Curvature	90 m	USGS (2006)
	Slope	90 m	USGS (2006)
	Aspect	90 m	USGS (2006)
	Hillshade	90 m	USGS (2006)
	MrVBF	90 m	USGS (2006)

(2009) explain in detail the mathematics of the equal-area spline.

By interpolating with this spline we obtained estimates of the concentration in the uppermost 30 cm of each profile (Fig. 1b). As our soil organic C values in 30 cm layer were positively skewed, we transformed the data to common logarithms ($\log_{10}$) before modelling.

3.2. Environmental covariates

The spatial distribution of the soil's organic C is controlled by a suite of environmental properties as they vary across the landscape. They include parent material, climate, biota and geomorphology. If the soil's C concentration is related closely to these factors and if data on them are easy to access then we might be able to map the C content of the soil efficiently and successfully (Zhou et al., 2016). We could obtain data on climate, vegetation, geology, and soil type and texture from public sources at several spatial resolutions (Table 1).

The Moderate Resolution Imaging Spectroradiometer (MODIS) provided us with information on a combination of land surface variables, and we obtained data on precipitation from the Tropical Rainfall Measuring Mission (TRMM), which is widely used in remote sensing applications. We also used the interpolated temperatures from meteorological stations provided by Data Center for Resources and Environmental Sciences of the Chinese Academy of Sciences (RESDC) (http://www.resdc.cn). In addition we had legacy data on soil texture, soil type, geology, type of vegetation and the Prescott index, which is a climate index related to soil formation (Prescott, 1950). The digital elevation model (DEM) at 90-m resolution (USGS, 2006) and the terrain factors derived from it across the whole of the Tibet provided us with the topographic information.

Apart from the terrain factors, all the other covariates were available only at coarser scales—see Table 1. To bring all the covariates to a common base we interpolated values of them from data to the same 90-m grid as that of the DEM by the nearest-neighbour method using ArcGIS 10.1 (Environmental Systems Research Institute, Inc., Redlands, CA, USA).

3.3. Mapping the organic C and its uncertainty

We used the regression-tree model Cubist of Quinlan et al. (1992) to predict the concentration of C with the environmental covariates across the whole of Tibet. The technique has been used effectively, and in particular for mapping soil over large areas by, for example, Viscarra Rossel and Chen (2011) and Mulder et al. (2016). Cubist is a form of piecewise linear regression. It partitions the covariates into several subsets with similar characteristics. The standard deviation, σ, in a given subset is used as a measure of the error at the node as splitting criterion. Each covariate at the same node is tested by estimation of the expected reduction in error. This splitting continues within each subset until there is no further reduction in the error or a few instances remain. The standard deviation reduction (SDR) is calculated as

$$\mathrm{SDR} = \sigma(P) - \sum_{i=1}^{N} \frac{|P_i|}{|P|}\sigma(P_i) \tag{3}$$

where P_i corresponds to the subsets after splitting the covariates, and P denotes the whole dataset.

Predictions are constructed with the linear regression model at the final node of the tree. When Cubist finally terminates the models, there is a list of rules and formulae. A set of rules obtained after the process with **if** and **else** define the partitions and prediction, and these rules are arranged in a hierarchy. Within each of the conditions, the model is formed as: **if** {conditions} then {linear formula}. A rule indicates that whenever a case satisfies the conditions of one rule, the corresponding linear formula is appropriate for predicting the value of the property to be predicted.

The following test serves as an example to illustrate the process.

If net primary productivity $< 434\,\mathrm{kg\ C\ m^{-2}}$
and evapotranspiration $> 255.9\,\mathrm{mm}$
and radiation $< 6.2\,\mathrm{kWh\ m^{-2}}$,
then the concentration of soil organic C = linear model.

Each group is determined by one or more variables; these are the rules, or conditions, for that group, and they depend on the spatial distribution of the associated variables. Within each group a linear regression model is built between the predictors and soil organic C.

We used the non-parametric bootstrap for estimating the distribution of the organic C predictions and to assess their uncertainties (Viscarra Rossel et al., 2014). This enabled us to take into account apparently random fluctuations arising from the sampling and in the predictors. We re-sampled from the model's predictions and from the predictors themselves. By repeated re-sampling and applying the bootstrap, in our case 50 times, we obtained 50 predicted values of the logarithm of C concentration at each point. These values were then

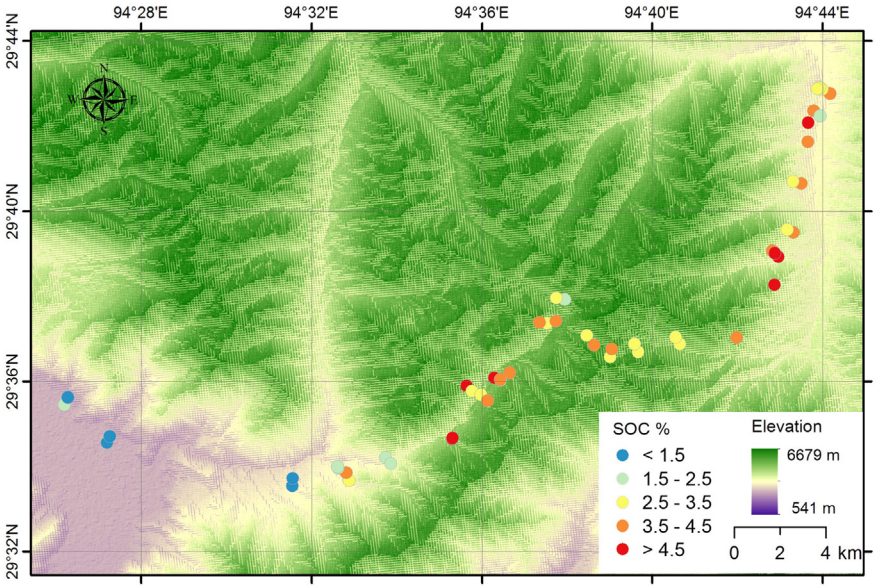

Fig. 2. The soil samples collected in Sygera Mountain between 2013 and 2015.

back-transformed to the original scale of concentration to provide a probability distribution for that point.

The final prediction was an average of the bootstrapped models. The uncertainty was quantified by the confidence interval at the 95% level. Each point on the grid was assigned to derive the upper and lower confidence limits of the interval. Finally, we expressed the uncertainty as

$$U = (C_{\text{upper}} - C_{\text{lower}})/C_{\text{mean}} \tag{4}$$

where C_{upper} and C_{lower} are the upper and lower 95% confidence limits for a grid, and C_{mean} was the average concentration of C obtained from the bootstrap. Calculations were performed using the R language for statistical computing (R Core Team, 2013) and package *Cubist* were used for modelling (Kuhn et al., 2014).

3.4. Calculation of stock of organic carbon

We calculated the stock of organic C in the uppermost 30 cm of soil as follows:

$$\text{STOCK} = \sum_{j=1}^{n} T_j \times D_j \times \text{SOC}_j \times (1 - C_j/100) \times R^2 \times 10^{-9} \tag{5}$$

where STOCK is the total stock of organic C (Pg), and for each of the n layers, $j = 1,2,\ldots,n$, T is its thickness (cm), D is its bulk density (g cm^{-3}), SOC is the concentration of C (%), C is the percentage of gravel (> 2 mm) and R is the resolution of map, which here is 90 m.

Records of bulk density and volumetric percentage of gravel in Tibet are few. We therefore calculated the bulk density using the empirical relation between soil organic C (SOC) and bulk density given by Wu et al. (2003) and is based on all the data recorded across China.

The relationship between soil C and bulk density is described in two regression equations, one for soil with less than 6% C and the other for soil soil with 6% or more:

$$\begin{aligned}&\text{Bulk density} = -0.1223\ln(\text{SOC}) + 1.290 \quad \text{for} \quad \text{SOC} < 6\%\\ &\text{Bulk density} = 1.377\exp(-0.0413 \times \text{SOC}) \quad \text{for} \quad \text{SOC} \geq 6\%.\end{aligned} \tag{6}$$

3.5. Model training and validation

We selected 191 (one-sixth) sample points randomly from the data for independent validation and used the remaining 957 points for calibration.

The assessment statistics we used for calibration, out-of-bag (OOB) validation and independent validation were the mean error (ME), the root mean square error (RMSE), the standard deviation of the error (SDE) and Lin's concordance correlation coefficient (CC) (Lin, 1989). These are respectively

$$\text{ME} = \frac{1}{N}\sum_{i=1}^{N}(\hat{y}_i - y_i) \tag{7}$$

$$\text{RMSE} = \sqrt{\frac{1}{N}\sum_{i=1}^{N}(\hat{y}_i - y_i)^2} \tag{8}$$

$$\text{SDE} = \sqrt{\frac{1}{N}\sum_{i=1}^{N}(\delta_i - \bar{\delta})^2}, \tag{9}$$

and

$$\text{CC} = \frac{2rs_{\hat{y}}s_y}{s_{\hat{y}}^2 + s_y^2 + (\bar{\hat{y}} - \bar{y})^2}. \tag{10}$$

In these equations y and $\hat{y}$ are the observed and predicted values of y, $\bar{y}$ and $\bar{\hat{y}}$ are the means of the observed and predicted y, δ is the difference between the observed and predicted values of y and $\bar{\delta}$ is the difference between the observed y and its mean, $\bar{y}$, s_y^2 and $s_{\hat{y}}^2$ are the variances of the observed and predicted y, r is the usual Pearson product-moment correlation coefficient between the observed and predicted values, and N is the number of comparisons.

The soil samples collected by the National Soil Survey were based on the soil taxonomy. So the samples are sporadic on the different soil types. We wanted an independent set of data for validation from different elevation to examine the elevational variation of our prediction, and the Sygera Mountain seemed a reasonable region to provide it. We know from the records of Yang et al. (2009) that the concentration of organic C in the soil of the Qinghai–Tibet grasslands has hardly changed since the 1980s, and we have every reason to believe that the same is true for Sygera Mountain. Soil samples had been collected by the National Soil Survey from sites representative of the Chinese soil taxonomy. From these we selected 32 sites spanning the altitudinal range from 2976 to 4523 m above sea level and measured the concentration of organic C in the uppermost 30 cm of the soil (Fig. 2) between 2013 and 2015. The data thus obtained were used to validate our predictions.

Table 2
Summary statistics for 0–30 cm layer soil organic carbon concentration of all the soil samples, training data for model, independent test data for validation and in Sygera.

	Number	Mean %	Standard deviation	Variance	Skewness	Minimum %	Maximum %	1st Quartile %	Medium	3rd Quartile %
All	1148	2.87	3.13	9.79	2.92	0.09	22.47	1.05	1.83	3.58
Training	957	2.85	3.07	9.44	2.92	0.09	22.47	1.07	1.81	3.55
Test	191	2.91	3.13	9.82	2.72	0.10	20.62	0.98	1.88	3.70
Sygera	32	3.59	1.37	1.94	0.61	0.83	6.85	2.76	3.51	4.35

Those soil organic C concentrations of these samples were then compared with those predicted by the method described above. We used the concordance correlation coefficients and root mean square error to assess the goodness of the predictions.

4. Results

4.1. Spatial modelling of C concentration

Table 2 summarizes the statistical distribution of the data. The data on C concentration were strongly positively skewed, and, as the above, we transformed the concentrations to their common logarithms to stabilize the variances. The mean concentration of organic C was 2.87% and its median was 1.83%. The mean organic C in Sygera was 3.59%, which is somewhat larger than that for the whole of Tibet.

Table 3 lists the model diagnostics of calibration and independent validation. The average of the concordance correlation coefficient for the 50 bootstraps of the calibration was 0.66, which is a little larger than 0.61 of the OOB validation and 0.63 of the independent validation. The 95% confidence limits of the concordance correlation coefficient were $C_{lower} = 0.64$ and $C_{upper} = 0.67$ for calibration and $C_{lower} = 0.62$ and $C_{upper} = 0.64$ for the independent validation (Table 3). Evidently the models constructed by Cubist were robust. The absolute mean error (ME) was much smaller than the standard deviation of the error (SDE) and made little contribution to the RMSE; the predictions were essentially unbiased.

We found that five environmental covariates contributed most in the conditions and regression for the models; Table 4 lists them. The ones that occur most frequently in the conditions are soil type, evapotranspiration (ET), precipitation from TRMM, vegetation type and radiation. They appear to control the distribution of organic C at the coarse scale. In contrast, temperature, net primary productivity (NPP), DEM and normalized difference vegetation index (NDVI), and also ET, appear in the regressions and affect the organic C at finer scales.

4.2. Mapping of soil organic carbon and its uncertainty

Fig. 3a shows the distribution of the predicted concentration of organic C in the topsoil of the whole of Tibet. It shows a trend decreasing from southeast to northwest. It matches the change in the climate from the humid montane zone at the head of the Brahmaputra River valley, where incidentally erosion is severe, via the somewhat drier, semi-humid, zone, still with fairly large concentrations of C, to the high, dry and cold Tibet Plateau proper where the sparse vegetation contributes little C to the soil.

Table 3
Model diagnostics for the calibration model, out-of-bag (OOB) and independent validation. The RMSE, ME and SDE are in $\log_{10}$(SOC)% unit.

		Mean	Upper 95% CL	Lower 95% CL
Calibration	CC_c	0.664	0.673	0.655
	$RMSE_c$	0.187	0.189	0.185
OOB validation	CC_o	0.611	0.620	0.602
	$RMSE_o$	0.199	0.202	0.197
	ME_o	−0.016	−0.012	−0.021
	SDE_o	0.199	0.202	0.196
Independent validation	CC_v	0.627	0.637	0.618
	$RMSE_v$	0.193	0.197	0.189
	ME_v	−0.012	−0.009	−0.016
	SDE_v	0.192	0.196	0.188

* CL is confidence limit.

Table 4
Average contribution (Top 5) of the environmental covariates occurs in the conditions and regression sections of the bootstrap models.

Rank	1	2	3	4	5
Condition environmental covariates	Soil type	ET	TRMM	Vegetation	Radiation
Contribution (%)	99	56	43	41	36
Regression environmental covariates	Temperature	ET	NPP	DEM	NDVI
Contribution (%)	91	87	84	77	69

The uncertainty in the predictions varies substantially. In part it depends on the density of the soil sampling. The greatest uncertainty is in the southwest of Tibet where sampling was sparsest. This high inhospitable part of Tibet is largely uninhabited and difficult to reach for field work (Fig. 3b). Sampling was sparse in the southeast of the country too, but the uncertainty of the predictions is somewhat less than in the southwest because the relationship between the C concentration and the environmental covariates was tighter.

Table 5 lists our predicted concentrations of C at a range of heights and for each climate zone. The mean concentration decreases with increasing height over the whole of Tibet. At one extreme, where the land surface lies below 3000 m above sea level, the mean concentration is 5.35%, while at the other in the soil on land above 5000 m, the mean concentration is only 1.46%, i.e. a quarter of that in the lowest land.

The whole of Tibet can be divided into four climatic zones (Fig. 1c), from humid in the southeast to dry in the northwest.

In the montane humid zone, plateau semi-humid zone and plateau frigid zone, the mean concentration of c decreases with increasing height (Table 5). In the montane humid and plateau semi-humid zone where the terrain varies intensely, the difference of C concentration between the lowest region and the highest is more than 2%, while in plateau frigid zone where the land is relatively flat, cold and dry, the difference is small. In the plateau cold temperate zone, covered mainly by steppe and meadow, the mean C concentration varies little regardless of elevation.

Table 6 lists our predictions of C for the main types of vegetation. For the grasslands, which include steppe and meadow and cover most of Tibet, there are big difference of mean concentrations of C between difference types. Under the subtropical tussock meadow the mean concentration is 4.45%, whereas under the temperate dwarf semi-shrub desert steppe the mean concentration is only 0.87%. The soil under rain forest in the southeast of Tibet has a mean concentration of nearly 6%. In contrast, the mean concentration of C in the desert is less than 1%. The concentration of C in the cropland soil is 3.86%, i.e. intermediate between the two extremes, but as the area is small it is of little consequence in carbon accounting.

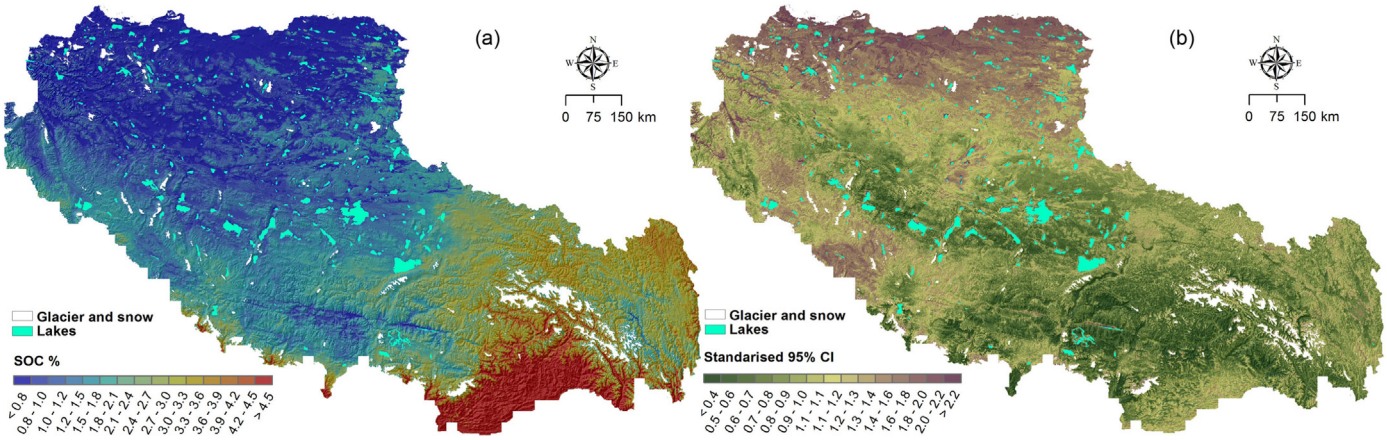

Fig. 3. Maps of (a) Tibet soil organic C concentration and (b) its uncertainty expressed in standardized form as the range of the 95% confidence intervals divided by its mean.

4.3. Independent validation of the soil organic C with the Sygera Mountain data

The concentration of C in the soil on Sygera Mountain varies with variation in height. We validated the predictions with soil samples there to be sure that we had correctly assigned values at the fine resolution. The value of the concordance correlation coefficient between the observed and predicted C is 0.67 and the RMSE is 0.89% (Fig. 4a).

4.4. Stock of organic C in the soil in Tibet

We estimated there to be 6.81 Pg of organic carbon in the uppermost 30 cm of the soil in Tibet within 95% confident limits of 3.80 Pg and 10.27 Pg (Table 7). The alpine steppe, with its vast area, contained most of the organic C, 1.93 Pg within the limits 0.83 Pg and 3.23 Pg (Fig. 5). The next largest contribution is in the meadow, 1.57 Pg with limits 0.89 Pg and 2.21 Pg. The soil of forests and shrub-land is relatively rich in organic C (Table 6), but it stocks much less C than the grasslands because these communities cover much smaller areas. The stocks of organic C in the soil are 0.66 Pg in coniferous forest, 0.63 Pg in broadleaf forest and 1.06 Pg under shrub (Fig. 5). The soil under alpine vegetation (Table 5) contains 0.89 Pg C. The soil of the alpine desert and that of the cropland contain the least amount of organic C, both less than 0.4 Pg (Fig. 5).

The soil of the semi-humid zone, with most of the shrub, alpine vegetation and some of the steppe and coniferous forest, contains 2.83 Pg C (within 95% confidence limits 1.73 and 3.98 Pg). The soil of plateau cold temperate zone, which is the largest climate zone in Tibet, contains 2.11 Pg C (within limits 1.13 and 3.24 Pg). The soil of the montane humid zone, dominated by forests, is estimated to contain

Table 5
Summary distribution of soil organic carbon and its 95% confidence intervals at different elevation gradient in Tibet and each climate zone.

	Elevation	Mean SOC %	Maximum %	Minimum %	SD %	Mean lower 95% CL	Mean upper 95% CL	Area (km^2)
Tibet	< 3000 m	5.35	8.48	0.16	1.07	2.90	7.82	57 405
	3000–3500 m	4.02	7.41	0.08	1.09	2.46	5.58	18 509
	3500–4000 m	3.10	6.92	0.18	1.21	1.89	4.32	43 505
	4000–4500 m	2.49	5.97	0.08	1.17	1.48	3.51	121 650
	4500–5000 m	1.61	5.88	0.02	0.92	0.86	2.59	481 306
	5000–5500 m	1.49	4.90	0.21	0.66	0.73	2.60	397 400
	> 5500 m	1.46	4.28	0.09	0.47	0.63	2.53	80 225
Montane humid	< 3000 m	5.52	8.48	0.16	0.88	2.97	8.07	51 044
	3000–3500 m	4.62	7.41	0.16	0.74	2.92	6.31	8133
	3500–4000 m	4.00	6.92	0.18	0.72	2.50	5.50	8915
	4000–4500 m	3.36	5.97	0.19	0.64	2.01	4.71	8589
	4500–5000 m	2.89	5.25	0.18	0.52	1.55	4.23	5094
	5000–5500 m	2.78	4.23	0.12	0.33	1.10	4.26	1509
	> 5500 m	2.68	3.53	0.09	0.24	0.80	4.76	537
Plateau semi-humid	< 3000 m	4.02	6.93	0.97	1.25	2.30	5.75	6314
	3000–3500 m	3.57	6.67	0.08	1.04	2.12	5.02	10 193
	3500–4000 m	2.90	6.57	0.18	1.19	1.76	4.04	33 857
	4000–4500 m	2.75	5.74	0.08	0.99	1.68	3.83	87 130
	4500–5000 m	2.48	5.88	0.10	1.17	1.41	3.56	138 355
	5000–5500 m	2.24	4.90	0.59	0.76	1.22	3.26	98 125
	> 5500 m	1.91	4.28	0.13	0.34	0.89	2.93	23 435
Plateau cold temperate	3000–3500 m	1.27	2.56	0.09	0.18	0.27	2.29	177
	3500–4000 m	1.50	3.69	0.39	0.83	0.57	2.57	731
	4000–4500 m	1.24	4.35	0.08	0.97	0.60	1.97	25 927
	4500–5000 m	1.35	4.32	0.02	0.69	0.70	2.09	262 683
	5000–5500 m	1.49	4.1	0.21	0.52	0.74	2.32	167 719
	> 5500 m	1.41	3.24	0.18	0.34	0.59	2.38	44 305
Plateau frigid	4500–5000 m	1.17	2.50	0.32	0.50	0.30	1.92	75 154
	5000–5500 m	1.11	2.52	0.36	0.44	0.27	2.01	130 025
	> 5500 m	1.09	2.46	0.23	0.38	0.22	1.98	11 930

* SD is standard deviation; CL is confidence limit.

Table 6
Summary distribution of soil organic carbon and its 95% confidence intervals at different elevation gradient in Tibet and each climate zone.

Vegetation subgroup	Mean SOC %	Maximum %	Minimum %	SD %	Mean lower 95% CI	Mean upper 95% CI	Area (km^2)
Subtropical coniferous forest	4.19	5.02	2.68	0.88	2.17	6.21	220
Subtropical montane coniferous forest	3.98	6.09	1.91	0.92	2.40	5.57	60 216
Subtropical deciduous broad-leaved forest	3.20	3.95	2.33	0.67	2.36	4.05	330
Subtropical evergreen broadleaf forest	5.47	7.96	2.32	0.93	2.99	7.94	27 851
Subtropical evergreen broadleaf sclerophyllous forest	3.95	4.11	3.88	0.16	2.61	5.29	330
Tropical rain forest	5.96	7.52	4.19	0.83	2.91	9.02	10 568
Subtropical deciduous broadleaf shrub	1.91	4.87	0.67	0.90	1.05	2.76	6715
Subalpine deciduous broadleaf shrub	2.29	4.69	0.83	0.89	1.27	3.31	16 072
Subalpine evergreen broadleaf shrub	3.28	6.26	1.57	0.69	1.91	4.66	80 581
Subalpine evergreen coniferous shrub	3.07	4.81	1.23	0.80	1.95	4.20	17 944
Semi-shrub desert	0.89	1.68	0.19	0.34	0.26	1.65	7376
Dwarf semi-shrub alpine desert	0.68	1.83	0.36	0.25	0.15	2.41	35 227
Temperate tussock grass steppe	1.79	3.49	0.69	0.63	1.18	5.81	15 852
Temperate dwarf semi-shrub desert steppe	0.87	2.11	0.29	0.33	0.41	1.45	37 428
Alpine steppe	1.11	3.31	0.34	0.43	0.52	2.12	472 037
Subtropical tussock meadow	4.45	5.43	1.32	1.56	3.08	5.81	551
Alpine wormwood meadow	2.13	4.17	0.51	0.68	1.14	3.12	243 614
Alpine cushion vegetation	1.62	2.49	0.86	0.49	0.72	2.71	1871
Alpine sparse vegetation	1.97	5.00	0.41	0.83	1.02	3.04	161 272
Crop	3.86	7.57	0.70	2.16	2.09	5.62	7486

1.11 Pg organic C. The soil of the high plateau frigid zone, part covered in alpine vegetation and part desert, where some parts are alpine and some are desert, is estimated to stock 0.77 Pg and makes the smallest contribution to the total (Fig. 5).

5. Discussion

5.1. Fine-resolution map of soil organic C in Tibet

The map of carbon concentration in the soil of the Tibetan Plateau made by the methods we describe from the several sources of data now available we believe to be an improvement of all previous maps. It covers the whole of Tibet and incorporates information on vegetation, soil type and climate. Despite the complexity of topography and the huge extent Cubist performed well, as judged by the matches between predictions and actual concentrations of organic C in the soil.

Our predictions differ somewhat from those of other investigations of soil C in Tibet. First, our study covers the whole of Tibet, whereas sparse sampling of the soil itself in the past has seriously limited the ability to map the soil of such a large area. We believe that by covering

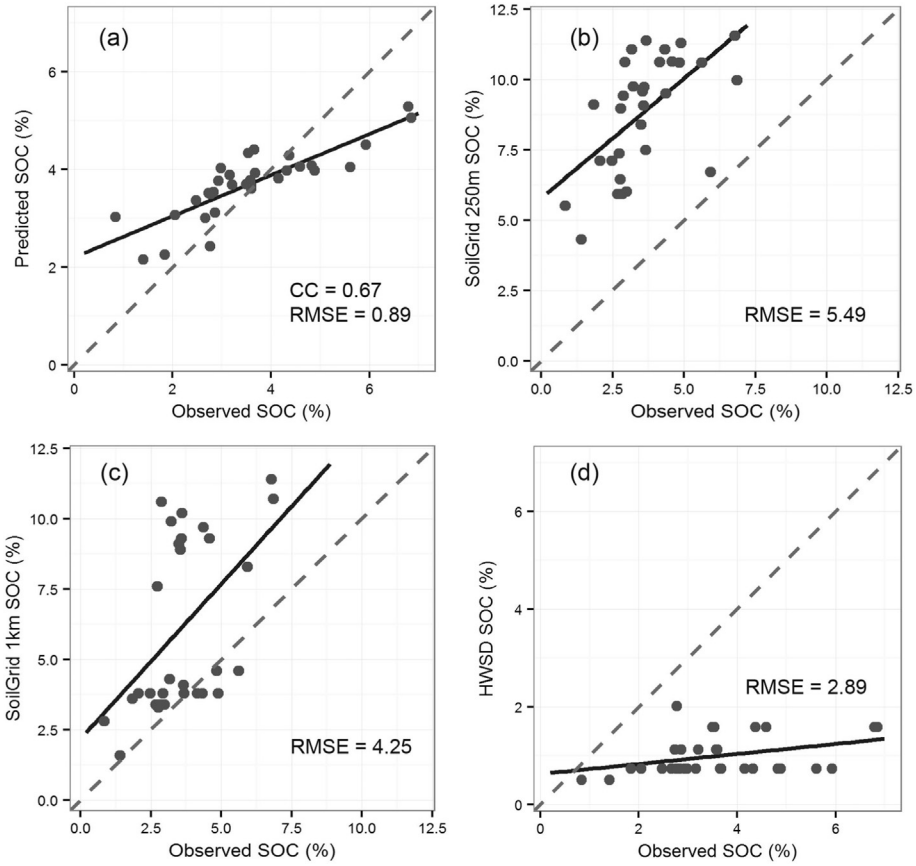

Fig. 4. Scatter plot of observed SOC with (a) predicted map, (b) SG1km, (c) SG250 m and (d) HWSD.

Table 7
Soil organic carbon storage of Tibet for sources of data and research.

Data	Organic C storage (Pg)	Lower 95% CL	Upper 95% CL
SoilGrids1 km	17.01		
SoilGrids250 m	13.61		
HWSD	7.58		
Fan et al. (2006)(0–20 cm)	4.69		
Our estimation	6.81	3.80	10.27

* SD is standard deviation; CL is confidence limit.

the whole of Tibet we get a better understanding of the variation than previously. Second, the 90-m resolution enables us to see local detail. For example, on the Sygera Mountain alone our map reveals differences of almost 6% in C concentration. More generally the fine resolution reveals the variation of soil C associated with differences in elevation, in which maps at coarser scales cannot do. The map of predictions helps to fill a gap in our knowledge of soil organic C on Qinghai–Tibet Plateau.

We recognize that predictions in the northwest of Tibet are accompanied by large uncertainties; that is almost inevitable where such sparse sampling produced rather little information on both the soil itself and the environmental covariates. In central and eastern Tibet, even though the terrain is more heterogeneous, the predictions were much more reliable because our sampling was denser (Fig. 3). Another likely reason for the large uncertainties in northwestern Tibet is that erosion redistributes even the small amounts of C there and produces spatial distributions that are at best only weakly related to environmental covariates (Yan et al., 2005; Li et al., 2008). Viscarra Rossel et al. (2014) found a similar situation in dry central Australia.

5.2. Comparison with the other existed data

We compared our map of predicted C concentration with SoilGrids with 1 km resolution (SG1 km), SoilGrids with 250 m resolution (SG250 m) and harmonized world soil database (HWSD) by computing the difference between them (Fig. 6).

Generally, the SG250 m of carbon concentration showed a spatial distribution with trend similar to ours. SoilGrids 1 km and HWSD, in contrast, differ substantially from ours. The differences between our predictions and the values of the SG250 m are significantly smaller than the differences of the SG1 km in most of Tibet. The biggest differences are in the southeast and southwest where the topography is rugged (Fig. 6f). The HWSD seems to underestimate the soil organic C in the east of Tibet and overestimate it in the west (Fig. 6d). It also shows relatively small values in the southeast under forest and subtropical meadows where we know that C concentration is large. Tifafi et al. (2018) investigated the performance of the SoilGrids and found that the SoilGrids overestimated soil organic C in the most boreal regions of those countries but did well at the more southerly latitudes where Tibet is located. Of course, they were not dealing with land at 4000 m and more, and perhaps not surprisingly therefore their results differed substantially from ours.

We also validated the estimates of these other maps with data on our samples from Sygera Mountain. We found that the SG250 m data overestimated the C there (Fig. 3b). In contrast, the HWSD data underestimated the true values, and there seemed to be no significant relation between the estimates of SG1 km and our observations (Fig. 3c). Generally, both the SG1 km and SG250 m grossly overestimated the C concentration.

The overestimation of soil organic C in Tibet by SoilGrids might be explained by weak or non-existent overall relations between C and the environmental covariates used in SoilGrids. For example, it is a general perception that the higher is the land the greater is the concentration of organic C in the soil—because the soil stays moist for longer thereby enabling plants to grow while decomposition is retarded by low temperature (Girardin et al., 2010; Dieleman et al., 2013). The relation is not monotonic, however: Tashi et al. (2016) found in the Himalayas in the south of the country that a positive correlation is held up to 3300 m. At higher elevation, and certainly above 4000 m, the relation is reversed, as shown by Ma et al. (2016). At some height between 3300 and 4000 m the cold climate limits plant growth more severely than it does decomposition, and so the organic C content of the soil decreases with increasing height (Garcia-Pausas et al., 2007). The samples from alpine areas are easy to be ignored in global models because so few samples have been collected there and the relatively small area in contrast with flat lands. Therefore we think that the global models such as SoilGrids are not appropriate to areas with specific exceptional conditions such as those of Tibet; a local model is needed instead.

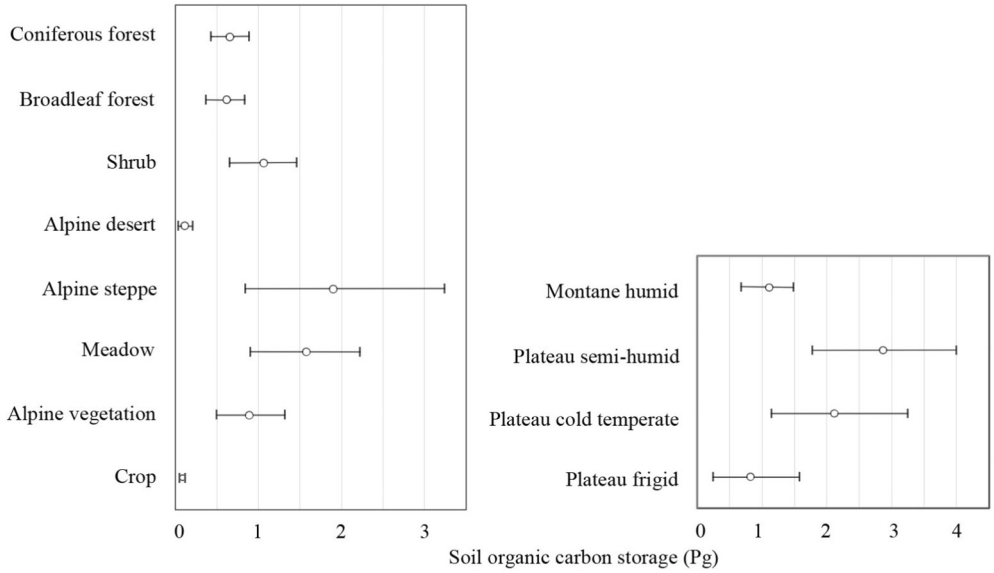

Fig. 5. Estimates of the storage of soil organic C of Tibet and its uncertainties expressed as 95% confidence intervals. The left one is divided by different vegetation type and the right one is divided by climate zone.

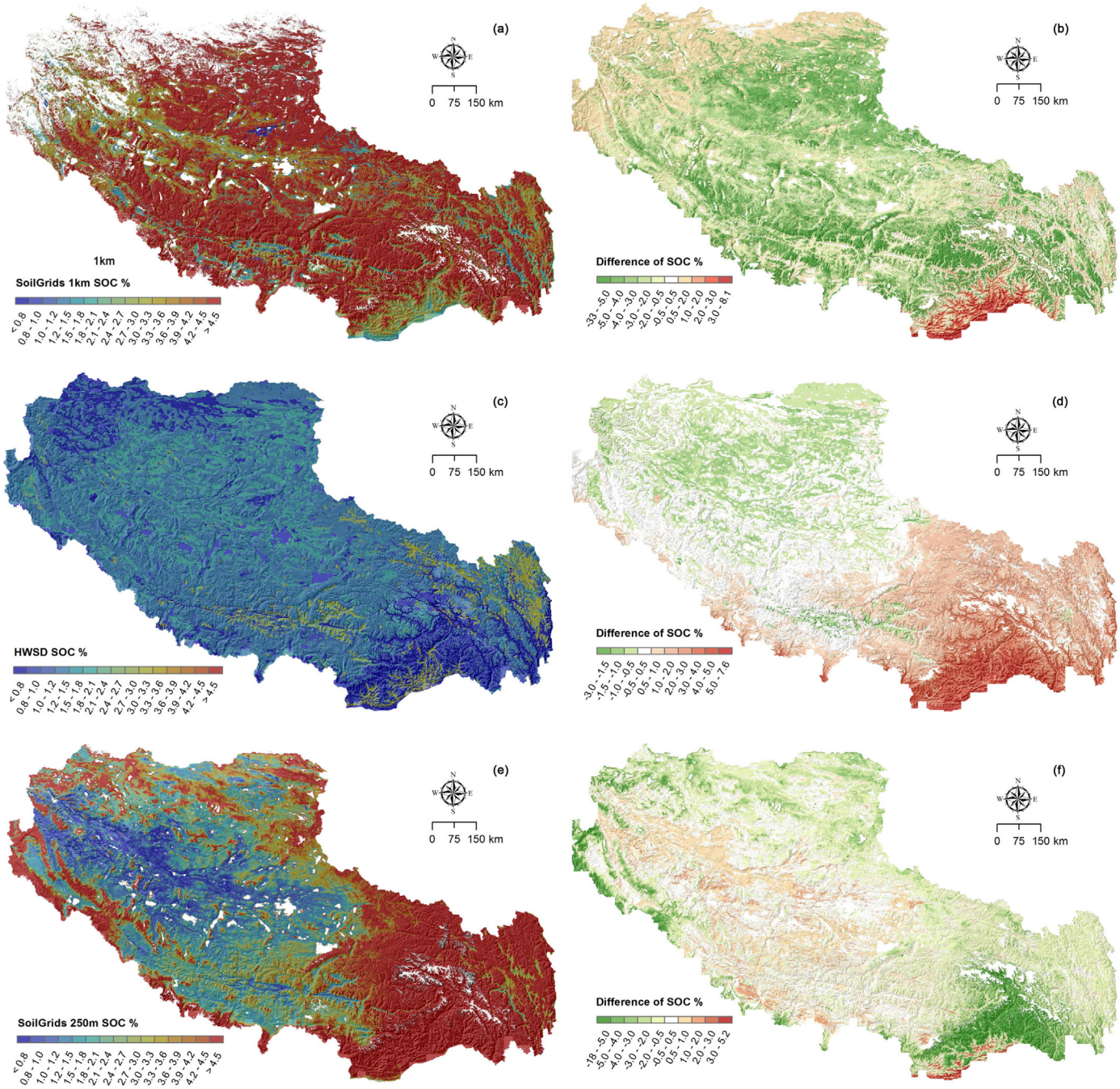

Fig. 6. The left three maps (a, c, e) are soil organic carbon for SoilGrids 1 km, HWSD and SoilGrids 250 m, respectively. The right three maps (b, d, f) are difference of soil organic carbon between the left three maps and our estimation. The colour green illustrated the data that were underestimated, the colour red illustrated the data that were overestimated compared with our estimation.

5.3. Implications for global understanding of soil organic C stock

Fan et al. (2006) estimated C stored in the uppermost 20 cm of soil to be 4.69 Pg, which is similar to our estimate (Table 7). That is not surprising because the two estimates are based on the same data. However, Fan et al. (2006) took soil subtype as the unit for the purpose of estimation, and so their estimate was less precise. The C storage estimated by SG1 km is as almost 3 times our estimate, and that of SG250 m is twice as large (Table 7). The difference between our estimate of C storage and that of HWSD is much smaller than SoilGrids. However, the HWSD showed no advantage over that of SoilGrids. The smaller difference in C storage between our estimate and that of of HWSD arises because overestimates of the HWSD are matched roughly by underestimates.

The uncertainty of our results is large; our confidence limits are 3.80 and 10.27 Pg, and they are wider than those for the stocks of organic C in the soil reported elsewhere (Cambule et al., 2014; Viscarra Rossel et al., 2014). One reason is that our sampling of Tibet is much sparser than those in other regions. A second reason is that the bulk densities, which are used in calculation of C stock from concentrations, were themselves predicted rather than measured, and so uncertainties in those predictions were propagated into the predictions of the C stocks. Both Schrumpf et al. (2011) and Tifafi et al. (2018) note that such inaccuracy in data on bulk density is a major source of uncertainty in the estimation of carbon stocks in soil. Evidently, to obtain accurate estimates of the soil's stock of organic C one must have accurate data not

only on the carbon concentration but also on the bulk density.

6. Conclusions

We can summarize our conclusions under three headings, as follows.

1. We now have reliable estimates of the amounts of organic stored in the soil of the Tibetan Plateau and of their spatial distribution, which we lacked previously. The map of estimates provides a baseline as it was in the 1980s for comparison with later maps and thereby to assess change in time. The total amount of carbon in the uppermost 30 cm of soil of the region is huge: 6.81 Pg. If only a small proportion were to be lost as CO_2 into the atmosphere as a result of global warming the consequences could be serious.
2. The Cubist method enabled us to combine dense data on environmental covariates with sparse soil data to predict and to map the carbon concentration at a fine geographic resolution. Its bootstrapping also enabled us to put confidence limits on the estimates and hence the uncertainties in the estimates. Thus, our 95% confidence limits on the total carbon were 3.80 and 10.27 Pg.
3. By following the route taken by Cubist through the data we can see which of the environmental covariates and climatic zones have the greatest influence on the predictions. That in turn leads to a better understanding of the relation between the soil and its environment in Tibet.

Acknowledgements

We acknowledge the financial support from the National Natural Science Foundation of China (nos: 41571339, 41461063). We also acknowledge the soil researchers who worked in the Tibetan Plateau and collected the precious samples during the National Soil Survey of China.

References

Arrouays, D., Grundy, M.G., Hartemink, A.E., Hempel, J.W., Heuvelink, G.B.M., Young Hong, S., Lagacherie, P., Lelyk, G., McBratney, A.B., McKenzie, N.J., Mendonc-Santos, M.d.L., Minasny, B., Montanarella, L., Odeh, I.O.A., Sanchez, P.A., Thomson, J.A., Zhang, G.L., 2014. Globalsoilmap: toward a fine-resolution global grid of soil properties. Adv. Agron. 125, 93–134.

Ballabio, C., 2009. Spatial prediction of soil properties in temperate mountain regions using support vector regression. Geoderma 151, 338–350.

Bishop, T.F.A., McBratney, A.B., Laslett, G.M., 1999. Modelling soil attribute depth functions with equal-area quadratic smoothing splines. Geoderma 91, 27–45.

Cambule, A.H., Rossiter, D.G., Stoorvogel, J.J., Smaling, E.M.A., 2014. Soil organic carbon stocks in the Limpopo National Park, Mozambique: amount, spatial distribution and uncertainty. Geoderma 213, 45–56.

Chinese Academy of Sciences, 2001. Vegetation Atlas of China. Science Press, Beijing.

Dieleman, W.I.J., Venter, M., Ramachandra, A., Krockenberger, A.K., Bird, M.I., 2013. Soil carbon stocks vary predictably with altitude in tropical forest: implications for soil carbon storage. Geoderma 204-205, 59–67.

Ding, J., Li, F., Yang, G., Chen, L., Zhang, B., Liu, L., Fang, K., Qin, S., Chen, Y., Peng, Y., Ji, C., He, H., Smith, P., Yang, Y., 2016. The permafrost carbon inventory on the Tibetan Plateau: a new evaluation using deep sediment cores. Glob. Chang. Biol. 22, 2688–2701.

Dörfer, C., Kühn, P., Baumann, F., He, J.S., Scholten, T., 2013. Soil organic carbon pools and stocks in permafrost-affected soils on the Tibetan Plateau. PLoS One 8 (2), e57024.

Fan, Y., Liu, S.Q., Zhang, S.R., Deng, L.J., 2006. Background organic carbon storage of topsoil and whole profile of soils from tibet district and their spatial distribution. Acta Ecol. Sin. 26, 2834–2846 (in Chinese with English abstract).

FAO/IIASA/ISRIC/ISSCAS/JRC, 2012. Harmonized World Soil Database (Version 1.2).FAO. IIASA, Rome.

Garcia-Pausas, J., Casals, P., Camarero, L., Huguet, C., Sebastià, J., Thomso, R., Romanyà, M.-T., 2007. Soil organic carbon storage in mountain grasslands of the Pyrenees: effects of climate and topography. Biogeochemistry 82, 279–289.

Girardin, C.A.J., Malhi, Y., Aragão, L.E.O.C., Mamani, M., Huarasca Huasca, W., Feeley, K.J., Rapp, J., Silva-Espejo, J.E., Silman, M., Salinas, N., Whittaker, R.J., 2010. Net primary productivity allocation and cycling of carbon along a tropical forest elevational transect in the Peruvian Andes. Glob. Chang. Biol. 16, 3176–3192.

Hengl, T., Mendes de Jesus, J., MacMillan, R.A., Batjes, N.H., Heuvelink, G.B.M., Ribeiro, E., Samuel-Rosa, A., Kempen, B., Leenaars, J.G.B., Walsh, M.G., Ruiperez Gonzalez, M., 2014. Soilgrids1 km: global soil information based on automated mapping. PLoS One 9 (8) E105992.

Hengl, T., Mendes de Jesus, J., Heuvelink, G.B.M., Ruiperez Gonzalez, M., Kilibarda, M., Blagotić, A., Shangguan, W., Wright, M.N., Geng, X., Bauer-Marschallinger, B., Antonio Guevara, M., Vargas, R., MacMillan, R.A., 2017. SoilGrids250 m: global gridded soil information based on machine learning. PLoS One 12 (2) E0169748.

Hoffmann, U., Hoffmann, T., Jurasinski, G., Glatzel, S., Kuhn, N.J., 2014. Assessing the spatial variability of soil organic carbon stocks in an alpine setting (Grindelwald, Swiss Alps). Geoderma 232-234, 270–283.

Kapos, V., Rhind, J., Edwards, M., Price, M., Ravilious, C., 2000. Developing a map of the world's mountain forests. In: Price, M.F., Butt, N. (Eds.), Forests in Sustainable Mountain Development: a State of Knowledge Report for 2000. CABI Publications, Wallingford, UK, pp. 4–19.

Kuhn, M., Weston, S., C., Keefer,Coulter, N., 2014. C Code for Cubist by Ross Quinlan (2014). Cubist: Rule- and Instance-Based Regression Modeling, R package version 0.0.15. . https://CRAN.R-project.org/package=Cubist.

Li, J., Okin, G.S., Alvarez, L., Epstein, H., 2008. Effects of wind erosion on the spatial heterogeneity of soil nutrients in two desert grassland communities. Biogeochemistry 88, 73–88.

Lin, L.I., 1989. A concordance correlation coefficient to evaluate reproducibility. Biometrics 45, 255–268.

Liu, W., Chen, S., Qin, X., Baumann, F., Scholten, T., Zhou, Z., Sun, W., Zhang, T., Ren, J., Qin, D., 2012. Storage, patterns, and control of soil organic carbon and nitrogen in the northeastern margin of the Qinghai-Tibetan Plateau. Environ. Res. Lett. 7 (3), 035401.

Lu, Y.M., Yue, T.X., Chen, C.F., Fan, Z.M., Wang, Q.M., 2010. Solar radiation modeling based on stepwise regression analysis in china. J. Remote Sens. 14, 858–884.

Ma, H.P., Yang, X.L., Guo, Q.Q., Zhang, X.J., Zhou, C.N., 2016. Soil organic carbon pool along different altitudinal level in the Sygera Mountains, Tibetan Plateau. J. Mt. Sci. 13, 476–483.

Ma, Z.Q., Shi, Z., Zhou, Y., Xu, J.F., Yu, W., Yang, Y.Y., 2017. A spatial data mining algorithm for downscaling TMPA 3B43 V7 data over the Qinghai–Tibet Plateau with the effects of systematic anomalies removed. Remote Sens. Environ. 200, 378–395.

Malone, B.P., McBratney, A.B., Minasny, B., Laslett, G.M., 2009. Mapping continuous depth functions of soil carbon storage and available water capacity. Geoderma 154, 138–152.

Mulder, V.L., Lacoste, M., Richer-de Forges, A.C., Martin, M.P., Arrouays, D., 2016. National versus global modelling the 3D distribution of soil organic carbon in mainland France. Geoderma 263, 16–34.

Nadeu, E., Gobin, A., Fiener, P., van Wesemael, B., van Oost, K., 2015. Modelling the impact of agricultural management on soil carbon stocks at the regional scale: the role of lateral fluxes. Glob. Chang. Biol. 21, 3181–3192.

NASA Land Processes Distributed Active Archive Center (LP DAAC), 2001. MODIS Land Products. In: USGS/Earth Resources Observation And Science (EROS) Center, Sioux Falls, South Dakota, USA.

Prescott, J.A., 1950. A climatic index for the leaching factor in soil formation. J. Soil Sci. 1, 9–19.

Quinlan, J., Adams, A., ASterling, L., 1992. Learning with continuous classes. In: AI'92: Proceedings of the 5th Australian Joint Conference on Artificial Intelligence. World Scientific, Singapore, pp. 343–348.

R Core Team, 2013. R: A Language and Environment for Statistical Computing. R Foundation for Statistical Computing, Vienna.

RESDC, 2016. Data Center for Resources and Environmental Sciences. Chinese Academy of Sciences. http://www.resdc.cn/data.aspx?DATAID=228.

Schrumpf, M., Schulze, E.D., Kaiser, K., Schumacher, J., 2011. How accurately can soil organic carbon stocks and stock changes be quantified by soil inventories? Biogeosciences 8, 723–769.

Shangguan, W., Dai, Y., Liu, B., Ye, A., Yuan, H., 2012. A soil particle-size distribution dataset for regional land and climate modelling in China. Geoderma 171-172, 85–91.

Shi, X.Z., Yu, D.S., Warner, E.D., Pan, X.Z., et al., 2004. Soil database of 1:1,000,000 digital soil survey and reference system of the Chinese Genetic Soil Classification System. Soil Surv. Horiz. 45, 111–148.

Tashi, S., Singh, B., Keite, C., Adams, M., 2016. Soil carbon and nitrogen stocks in forests along an altitudinal gradient in the eastern Himalayas and a meta-analysis of global data. Glob. Chang. Biol. 22, 2255–2268.

Tifafi, M., Guenet, B., Hatté, C., 2018. Large differences in global and regional total soil carbon stock estimates based on SoilGrids, HWSD, and NCSCD: intercomparison and evaluation based on field data from USA, England, Wales, and France. Global Biogeochem. Cycles 32, 42–56.

USGS, 2006. Shuttle Radar Topography Mission, 1 Arc Second scenes. In: Global Land Cover Facility. University of Maryland, Maryland, US.

Viscarra Rossel, R.A., Chen, C., 2011. Digitally mapping the information content of visible-near infrared spectra of surficial Australian soils. Remote Sens. Environ. 115, 1443–1455.

Viscarra Rossel, R.A., Webster, R., Bui, E., Baldock, J.A., 2014. Baseline map of organic carbon in Australian soil to support national carbon accounting and monitoring under climate change. Glob. Chang. Biol. 20, 2953–2970.

Ward, A., Dargusch, P., Thomas, S., Liu, Y., Fulton, E.A., 2014. A global estimate of carbon stored in the world's mountain grasslands and shrublands, and the implications for climate policy. Glob. Environ. Chang. 28, 14–24.

Wu, H., Guo, Z., Peng, C., 2003. Land use induced changes of organic carbon storage in soils of China. Glob. Chang. Biol. 9, 305–315.

Yan, H., Wang, S., Wang, C., Zhang, G., Patel, N., 2005. Losses of soil organic carbon under wind erosion in China. Glob. Chang. Biol. 11, 828–840.

Yang, R.M., Zhang, G.L., Yang, F., Zhi, J., Yang, F., Liu, F., Li, D., 2016. Precise estimation of soil organic carbon stocks in the northeast Tibetan Plateau. Sci. Rep. 6, 21842.

Yang, Y., Fang, J., Tang, Y., Ji, C., Zheng, C., He, J., Zhu, B., 2008. Storage, patterns and controls of soil organic carbon in the Tibetan grasslands. Glob. Chang. Biol. 14, 1592–1599.

Yang, Y.H., Fang, J.Y., Smith, P., Tang, Y.H., Chen, A.P., Ji, C.J., Hu, H.F., Rao, S., Tan, K., He, J.S., 2009. Changes in topsoil carbon stock in the Tibetan grasslands between the 1980s and 2004. Glob. Chang. Biol. 15, 2723–2729.

Zhou, Y., Biswas, A., Ma, Z., Lu, Y., Chen, Q., Shi, Z., 2016. Revealing the scale-specific controls of soil organic matter at large scale in northeast and north China plain. Geoderma 271, 71–79.